# Resonant inelastic x-ray scattering studies of elementary excitations

Ament, L.J.P.

# Chapter 7

# Phonon RIXS

Unpublished work. *Determining the Electron-Phonon Coupling Strength in Correlated Electron Systems from Resonant Inelastic X-ray Scattering*, with Michel van Veenendaal and Jeroen van den Brink.

## 7.1 Introduction

Often novel electronic properties of materials can be understood by systematically unravelling the interaction between its electrons and phonons. Tunable electric transport properties in molecular crystals, for instance, are explained by the presence of a strong electron-phonon (e-p) coupling [225]. The dressing of electrons by phonons is also responsible for the colossal magnetoresistance effect in manganites [226]. More delicate is the role that the e-p interaction plays in high-$T_c$ superconducting cuprates, which is the topic of a hot, persisting debate [227–229]. The lack of a technique to measure the e-p coupling strength perpetuates this controversy. Here we show that high resolution RIXS fills this void and can provide direct, element-specific and momentum-resolved information on the coupling between electrons and phonons. We provide the theoretical framework required to distill e-p interaction strengths from RIXS, particularly in strongly correlated transition metal oxides such as the high-$T_c$ cuprates.

The state-of-the-art resolution of RIXS experiments is such that photon energy loss features on an energy scale of 25 meV can be distinguished at a copper or nickel $L_3$ edge [11,112]. This resolution has brought phonons within the energy window of observation and indeed this year the first glimpses of phonons were resolved in RIXS [11, 230]. To put this achievement in perspective, one should

realize that the incident photons at the Cu L edge have an energy of around 930 eV, implying experiments have a resolving power of about $4 \cdot 10^4$. Developments in instrumentation are driving this already impressive figure further up [3]. Here we show how the progress in accuracy will allow the extraction of a number of characteristics of the e-p interaction directly from RIXS, including spatial information on the e-p coupling strength. No other experimental technique has access to such e-p characteristics, particularly in strongly correlated 3d transition metal oxides.

RIXS couples to phonons because the intermediate state in the RIXS process has an altered charge distribution, which influences the lattice. Most core holes decay very rapidly, and there is not enough time for the lattice to fully adjust to the transient charge distribution. Therefore, the final states of the RIXS process contain only few phonons; multi-phonon excitations are suppressed by the large lifetime broadening $\Gamma$.

The advantage of RIXS is that X-ray photons carry an appreciable momentum. This allows RIXS to sample the Brillouin zone and hence the phonon dispersion. In contrast, Raman scattering in the optical range is restricted to zero momentum transfer. Using Raman or neutron scattering, one can measure the broadening of phonon peaks. Because of e-p coupling, the phonon decays for instance in an electron-hole pair and consequently the lifetime of the phonon is decreased. This adds to the broadening of the phonon peaks. Allen's formula [231] gives the connection between this broadening and the e-p coupling constant. However, in the absence of low energy electron-hole excitations, like in Mott insulators, this decay channel does not exist. Other methods to measure the e-p interaction also do not have access to momentum-dependent information. Electron tunneling for instance, has no momentum-dependence and thus cannot probe how strong an electron couples to a particular phonon at a particular wavevector. Moreover, it is intrinsically surface sensitive and suffers from the practical difficulty to make good yet partially transparent barriers [232–234]. Another asset of RIXS is its element-specificity: in a cuprate not only the copper-related phonons can in principle be accessed at the Cu L edge, but also the oxygen-related ones at the O K edge – resolution permitting.

Measuring phonon dispersions is a promising new utilization of RIXS but as a technique it is up against inelastic neutron scattering and (non-resonant) inelastic X-ray scattering, well-established experimental methods with the same capacity. Here we make the case that what really sets RIXS apart is the way phonons are excited, leading to the capability to measure momentum dependent e-p couplings.

This chapter is organized as follows: Sec. 7.2 reviews the general e-p coupling Hamiltonian and how it relates to RIXS. In Sec. 7.3, the cross sections for Einstein phonons and dispersive phonons are derived. These yield complicated expressions, which simplify tremendously in the UCL expansion, as explained in Sec. 7.3.1.

## 7.2 Electron-phonon coupling

As an introduction to phonon scattering in RIXS, we start with a summary of e-p coupling, closely following chapter 1.3.2 in Ref. [62]. Then we discuss how the e-p Hamiltonian relates to the RIXS process, where the core hole and the photo-excited electron form a potential that perturbs the lattice.

### 7.2.1 Theory of electron-phonon coupling

We will assume that the core hole binds the photo-excited electron (which is a very good approximation at the Cu L edge [157]). The electron-phonon Hamiltonian for electrons localized at positions $\mathbf{R}_i$ is [62]

$$H = \sum_{\mathbf{k},\lambda} \left[ \omega_{\mathbf{k}\lambda} b^\dagger_{\mathbf{k},\lambda} b_{\mathbf{k},\lambda} + \sum_i \left( b_{\mathbf{k},\lambda} + b^\dagger_{-\mathbf{k},\lambda} \right) e^{i\mathbf{k}\cdot\mathbf{R}_i} \sum_{\mathbf{G}} \mathcal{M}_{\mathbf{k}+\mathbf{G},\lambda} \eta(\mathbf{k}+\mathbf{G}) e^{i\mathbf{G}\cdot\mathbf{R}_i} \right] \tag{7.1}$$

The free phonon dynamics is governed by the first term. The second term of the Hamiltonian couples the electrons to phonons with momentum $\hbar\mathbf{k}$ and branch index $\lambda$, which are created by the operator $b^\dagger_{\mathbf{k}\lambda}$. Note that we have chosen units such that $\hbar = 1$. Further, we have

$$\mathcal{M}_{\mathbf{k}+\mathbf{G},\lambda} = -(\mathbf{k}+\mathbf{G}) \cdot \boldsymbol{\xi}_{\mathbf{k}\lambda} \sqrt{\frac{\hbar}{2\rho\mathcal{V}\omega_{\mathbf{k}\lambda}}} V_{ei}(\mathbf{k}+\mathbf{G}) \tag{7.2}$$

$$\eta(\mathbf{k}+\mathbf{G}) = \int d\mathbf{r} e^{i(\mathbf{k}+\mathbf{G})\cdot\mathbf{r}} \Delta\rho(\mathbf{r}) \tag{7.3}$$

with $\Delta\rho(\mathbf{r})$ the change in the charge distribution due to the electron (centered at $\mathbf{r} = \mathbf{0}$), $\mathcal{V}$ the volume of the crystal and $\rho$ its density. $\boldsymbol{\xi}_{\mathbf{k}\lambda}$ is the phonon polarization. $V_{ei}(\mathbf{k})$ is the Fourier transform of the potential of an ion placed at the origin. For an ion with a point-potential, $V_{ei}(\mathbf{k}) \propto 1/\mathbf{k}^2$.

We assume that the crystal has inversion symmetry: $\omega_{\mathbf{k}\lambda} = \omega_{-\mathbf{k},\lambda}$ and $\boldsymbol{\xi}_{\mathbf{k}\lambda} = -\boldsymbol{\xi}^*_{-\mathbf{k},\lambda}$. Since the Hamiltonian should be Hermitian, we obtain the condition $\mathcal{M}^*_{-\mathbf{k}-\mathbf{G},\lambda}\eta^*(-\mathbf{k}-\mathbf{G}) = \mathcal{M}_{\mathbf{k}+\mathbf{G},\lambda}\eta(\mathbf{k}+\mathbf{G})$, which is indeed satisfied if $V^*_{ei}(-\mathbf{k}-\mathbf{G}) = V_{ei}(\mathbf{k}+\mathbf{G})$: $V_{ei}$ is invariant under inversion too.

Next, we assume that there is only one electronic excitation during the RIXS process, as is the case in RIXS if we neglect the electronic intermediate state dynamics. The unit cell is chosen such that the core hole is located at its center ($\mathbf{R}\cdot\mathbf{G} = 0$).

The electronic degree of freedom can be written in second quantization, using $e^{i\mathbf{k}\cdot\mathbf{R}} = \sum_i d^\dagger_i d_i e^{i\mathbf{k}\cdot\mathbf{R}_i}$ where $d_i$ annihilates the photo-excited electron at site $i$. In momentum space, the Hamiltonian is

$$H = \sum_{\mathbf{k},\lambda} \left[ \omega_{\mathbf{k}\lambda} b^\dagger_{\mathbf{k}\lambda} b_{\mathbf{k}\lambda} + M_{\mathbf{k}\lambda} \sum_{\mathbf{p}} d^\dagger_{\mathbf{p}} d_{\mathbf{p}-\mathbf{k}} \left( b_{\mathbf{k}\lambda} + b^\dagger_{-\mathbf{k},\lambda} \right) \right] \tag{7.4}$$

with

$$M_{\mathbf{k}\lambda} = \sum_{\mathbf{G}} \mathcal{M}_{\mathbf{k}+\mathbf{G},\lambda}\eta(\mathbf{k}+\mathbf{G}). \tag{7.5}$$

Because of inversion symmetry $M^*_{\mathbf{k},\lambda} = M_{-\mathbf{k},\lambda}$.

### 7.2.2 Electron-phonon coupling in RIXS

To understand the capacity of RIXS to measure the momentum dependence of the e-p interaction, we start with the e-p coupling Hamiltonian (7.4). For definiteness we focus on the high-$T_c$ cuprates which have all their Cu 3d orbitals filled apart from a single hole in the $x^2$-$y^2$ orbitals, but our analysis is general. In the Cu L edge RIXS process, the $x^2$-$y^2$ state is transiently occupied as an electron from the core is launched into it. The change in the charge density $\Delta\rho(\mathbf{r})$ is given by the shape of the $x^2$-$y^2$ orbital and the core hole. As mentioned before, the filled $x^2$-$y^2$ state is very short-lived. There is then a certain probability that during the lifetime of the core hole a phonon is excited and left behind in the final state. Obviously this probability is related to the coupling of the $x^2$-$y^2$ electron to this particular phonon. Note that the presence of the core hole ensures that the intermediate state is locally charge neutral. Thus the phonons that couple to the 3d $x^2$-$y^2$ state with its characteristic quadrupolar charge distribution light up in L edge RIXS.

One might object that the phonons react to the core hole as well as to the photo-excited electron. The contribution of the core hole to the electric potential outside the Cu ion is very small, however, as can be seen from a multipole expansion of the potential of the core hole plus photo-excited electron (see, for instance, Ref. [235], page 148):

$$V(\mathbf{r}) = \frac{1}{4\pi\epsilon_0}\left[\frac{1}{r}\int d\mathbf{r}'\ \rho(\mathbf{r}') + \frac{1}{r^2}\int(\hat{\mathbf{r}}\cdot\mathbf{r}')\rho(\mathbf{r}') + \frac{1}{2r^3}\int d\mathbf{r}'[3(\hat{\mathbf{r}}\cdot\mathbf{r}')^2 - \mathbf{r}'^2]\rho(\mathbf{r}') + \ldots\right] \tag{7.6}$$

where $\mathbf{r} = |\mathbf{r}|\hat{\mathbf{r}} = r\hat{\mathbf{r}}$ and $\rho(\mathbf{r}) = e\,|\langle\mathbf{r}|\,2p\rangle|^2 - e\,|\langle\mathbf{r}|\,3d\rangle|^2$, with $|2p\rangle$ and $|3d\rangle$ the states of the core hole and the photo-excited electron, respectively. Since the core orbitals have a very small radius compared to the valence orbitals, a first order approximation would be $|\langle\mathbf{r}|\,2p\rangle|^2 \approx \delta(\mathbf{r})$, and the core hole only contributes to the monopole of the potential. Outside the Cu ion, the total monopole contribution vanishes. Within this approximation, the only contributions to the electric potential outside the Cu ion come from the 3d valence orbitals. Further, the dipole contributions are zero by symmetry. We conclude that the lattice couples mainly to the quadrupole potential of the photo-excited electron, and not to the core hole. At the Cu $K$-edge, in contrast, the main contribution to the potential comes from the core hole.

## 7.3 RIXS cross section for phonons

To understand how the electron-phonon coupling is precisely reflected in the RIXS intensity, we evaluate the RIXS amplitude for phonon scattering $\mathcal{F}$ in the Kramers-Heisenberg equation (2.30). The polarization factor (2.42) describing processes where only phonons are excited, is well approximated by the elastic process, as the phonons modify the electronic states of the system only slightly. Consequently, the dipole transition amplitudes are also marginally affected. In the case of Cu L edge RIXS at the cuprates, the photo-excited electron fills the only available hole, *i.e.*, the hole in the $3d_{x^2-y^2}$ orbital. The polarization factor for elastic processes and phonon scattering is given by

$$T_\psi(\boldsymbol{\epsilon}', \boldsymbol{\epsilon}) = \langle\psi|\, \boldsymbol{\epsilon}'^* \cdot \mathbf{r} \left|3d_{x^2-y^2}\right\rangle \left\langle 3d_{x^2-y^2}\right| \boldsymbol{\epsilon} \cdot \mathbf{r}\, |\psi\rangle \tag{7.7}$$

where $\psi$ is one of the resonant core states, see, *e.g.*, Sec. 4.3.1. Since the lattice (approximately) does not react to the core hole, the latter can be integrated out from the scattering amplitude:

$$\mathcal{F}_{fi} = \sum_\psi T_\psi(\boldsymbol{\epsilon}', \boldsymbol{\epsilon}) \sum_i e^{i\mathbf{q}\cdot\mathbf{R}_i} \sum_n \frac{\langle f|\, d_i\, |n\rangle \langle n|\, d_i^\dagger\, |i\rangle}{E_i + \hbar\omega_\mathbf{k} - E_n + i\Gamma}. \tag{7.8}$$

The sum over $\psi$ can be performed and gives the atomic scattering factor for elastic scattering $T_{\mathrm{el}}(\boldsymbol{\epsilon}', \boldsymbol{\epsilon}) = \sum_\psi T_\psi(\boldsymbol{\epsilon}', \boldsymbol{\epsilon})$.

Due to the presence of the intermediate states, it is in general impossible to evaluate RIXS scattering intensities exactly, even in model systems. One therefore often resorts to finite size cluster calculations to compute RIXS spectra [2,73]. The e-p problem at hand, however, is an exception. We have solved the RIXS phonon spectrum exactly by means of a canonical transformation. The fact that one is dealing with harmonic bosons allows for this solution.

**Einstein phonons.** In analyzing the general solution, it is instructive to consider the Einstein model, which comprises a single non-dispersive phonon per site of frequency $\omega_0$ with a coupling strength $M$. The e-p Hamiltonian reduces to

$$H = \sum_i \omega_0 b_i^\dagger b_i + M d_i^\dagger d_i (b_i^\dagger + b_i). \tag{7.9}$$

This Hamiltonian can be diagonalized by a canonical transformation $\bar{H} = e^S H e^{-S}$ [62], with $S = \sum_i d_i^\dagger d_i S_i$ where

$$S_i = \frac{M}{\omega_0}(b_i^\dagger - b_i). \tag{7.10}$$

As there is a single core hole present, this results in

$$\bar{H} = \sum_i \omega_0 b_i^\dagger b_i - \frac{M^2}{\omega_0}, \tag{7.11}$$

where the last term merely shifts the energy at which the resonance occurs. The eigenstates of $\bar{H}$ are all the possible occupations $\{n_i\}$ of the phonon states, indexed by $m$, with energies $E_m = \sum_i n_i(m)\omega_0 - M^2/\omega_0$. The transformation can be thought of as shifting the origin of the lattice coordinate to the new equilibrium position of the lattice: zero phonons in a transformed state describes the lattice at rest in the new equilibrium position. The eigenstates $\left|\bar{\psi}_m\right\rangle$ of $\bar{H}$ are related to the eigenstates $|\psi_m\rangle$ of $H$ by $|\psi_m\rangle = e^{-S}\left|\bar{\psi}_m\right\rangle$. Inserting this transformation in the scattering amplitude (7.8) gives

$$\begin{aligned}\mathcal{F}_{fi} &= T_{\mathrm{el}}(\boldsymbol{\epsilon}', \boldsymbol{\epsilon}) \sum_i e^{i\mathbf{q}\cdot\mathbf{R}_i} \sum_m \frac{\langle f|\, d_i\, e^{-S}\left|\bar{\psi}_m\right\rangle \left\langle\bar{\psi}_m\right| e^{S} d_i^\dagger\, |i\rangle}{E_i + \hbar\omega_{\mathbf{k}} - E_m + i\Gamma} \\ &= T_{\mathrm{el}}(\boldsymbol{\epsilon}', \boldsymbol{\epsilon}) \sum_i e^{i\mathbf{q}\cdot\mathbf{R}_i} \sum_{n_i=0}^{\infty} \frac{\langle n_i'|\, e^{-S_i}\, |n_i\rangle \langle n_i|\, e^{S_i}\left|n_i^0\right\rangle}{z + M^2/\omega_0 - n_i\omega_0}, \end{aligned} \tag{7.12}$$

where in the last step the photo-excited electron degree of freedom is integrated out. We defined $z = \hbar\omega_{\mathbf{k}} - E_{\mathrm{res}} + i\Gamma$, where $E_{\mathrm{res}}$ is the peak energy of the phonon-broadened XAS spectrum (see page 226 of Ref. [62]). $n_i^0$, $n_i$, and $n_i'$ are the occupations in the initial, intermediate, and final states, respectively. In the local model, the final states are indexed by the local phonon numbers $\{n_i'\}$. Note that final states where the phonon number has been changed at multiple sites cannot be reached: phonons can only be created and annihilated at the core hole site, and only contributions from this site remain in the numerator of Eq. (7.12).

The evaluation of the scattering amplitude is given in appendix C; the zero temperature result is

$$\mathcal{F}_{fg} = T_{\mathrm{el}}(\boldsymbol{\epsilon}', \boldsymbol{\epsilon}) \sum_i e^{i\mathbf{q}\cdot\mathbf{R}_i} \left[\sum_{n=0}^{n_i'} \frac{B_{n_i' n}(g) B_{n0}(g)}{z + (g-n)\omega_0} + \sum_{n=n_i'+1}^{\infty} \frac{B_{n n_i'}(g) B_{n0}(g)}{z + (g-n)\omega_0}\right], \tag{7.13}$$

with $g = M^2/\omega_0^2$. The Franck-Condon (FC) factors in the numerator are

$$B_{ab}(g) = \sqrt{e^{-g} a!\, b!} \sum_{l=0}^{b} \frac{(-1)^a (-g)^l \sqrt{g}^{a-b}}{(b-l)!\, l!\, (a-b+l)!}. \tag{7.14}$$

The zero temperature RIXS cross section is obtained by squaring the amplitude. As argued above, final states where the phonon number has changed at multiple sites cannot be reached with local phonons, so the sum over final states in the Kramers-Heisenberg equation is $\sum_i \sum_{n_i'=0}^{\infty}$. We get for the cross section

$$\begin{aligned}\frac{d^2\sigma}{d\Omega d\omega} \propto \sum_f |\mathcal{F}_{fg}|^2\, \delta(\omega - n'\omega_0) = N\, |T_{\mathrm{el}}(\boldsymbol{\epsilon}', \boldsymbol{\epsilon})|^2 \sum_{n'=0}^{\infty} \Bigg| \sum_{n=0}^{n'} \frac{B_{n'n}(g) B_{n0}(g)}{z + (g-n)\omega_0} \\ + \sum_{n=n'+1}^{\infty} \frac{B_{nn'}(g) B_{n0}(g)}{z + (g-n)\omega_0} \Bigg|^2 \delta(\omega - n'\omega_0) \end{aligned} \tag{7.15}$$

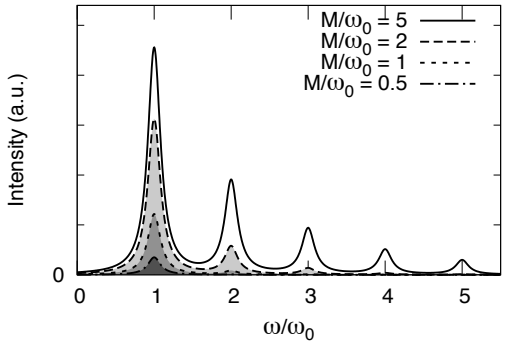


**Figure 7.1:** RIXS phonon cross section for Einstein phonons with energy $\omega_0$, for different electron-phonon couplings $M$. We take $\Gamma/\omega_0 = 5$ (a typical value at the copper L edge), and an incident energy corresponding to the maximum in the XAS signal. The polarization dependence is omitted in this plot, as well as the zero loss peak, which shifts to the Bragg peaks in an ideal crystal.

Note that the $\mathbf{q}$ dependence is lost, because of the local nature of the Einstein phonons.

The resulting RIXS spectra for a typical weak, intermediate and strong coupling case are shown in Fig. 7.1. It is clear that for stronger e-p interactions, a larger number of multi-phonon satellites carry appreciable weight.

However, the first important observation is that the intensity of the zero loss peak is dominant even in the strong e-p coupling regime, as is clear from Figs. 7.2 and 7.3. Its spectral weight is larger than the weight of all phonon loss peaks combined when $M/\Gamma \lesssim 1.5$. As at the Cu $L_3$ edge $\Gamma = 280$ meV [100], this corresponds to the physical situation. This observation is empirically supported by the fact that a dispersion of magnon [11, 19, 21] and bimagnon [14, 51–53] excitations has been observed in L and K edge RIXS. Such dispersion would be absent if these magnetic excitations were always accompanied by (multiple) phonons, see Sec. 7.4.

It is interesting to note that in the case of an infinitely fast scattering process ($\Gamma \to \infty$), the lattice has no time to react to the transient electronic excitation, and no phonons are excited in the final state.

The exact intensity for exciting a single phonon in the RIXS process is

$$I^{(1)} = N\,|T_{\rm el}(\boldsymbol{\epsilon}', \boldsymbol{\epsilon})|^2\,\frac{e^{-2g}}{g}\left|\sum_{n=0}^{\infty}\frac{g^n(n-g)}{n!(z+(g-n)\omega_0)}\right|^2, \tag{7.16}$$

In leading order in the e-p coupling $g$ this is $I^{(1)} \approx N|T_{\rm el}(\boldsymbol{\epsilon}', \boldsymbol{\epsilon})|^2 M^2/|z|^4$ so that in this limit the single-phonon RIXS scattering intensity is directly proportional to the dimensionless e-p coupling constant $g$, see Fig. 7.3. Increasing $z$ by tuning away from the absorption edge reduces the single-phonon scattering intensity.

Even when the e-p coupling $g$ is not small, we can obtain the RIXS amplitude in approximate form by using the fact that the timescale of a typical phonon (80 meV $\sim$ 52 fs) is much slower than the ultrashort RIXS timescale (1.6 eV $\sim$ 2.6 fs at the Cu K edge). This separation of timescales suggests that the scattering

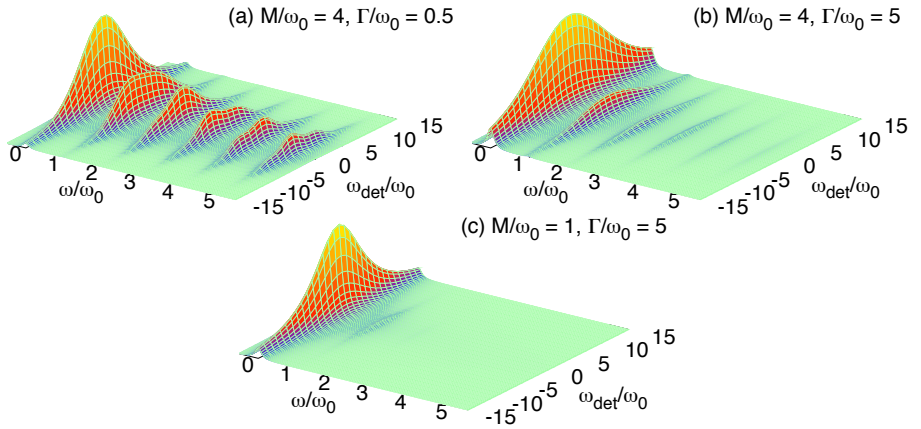


**Figure 7.2:** Calculated RIXS intensities for phonon loss as a function of loss energy $\omega$ and detuning from the maximum of the absorption spectrum $\omega_{\rm det} = \mathfrak{Re}\{z\}$ in the case of (a) strong coupling and very long core-hole lifetime, (b) strong e-p coupling and (c) intermediate/weak e-p coupling.

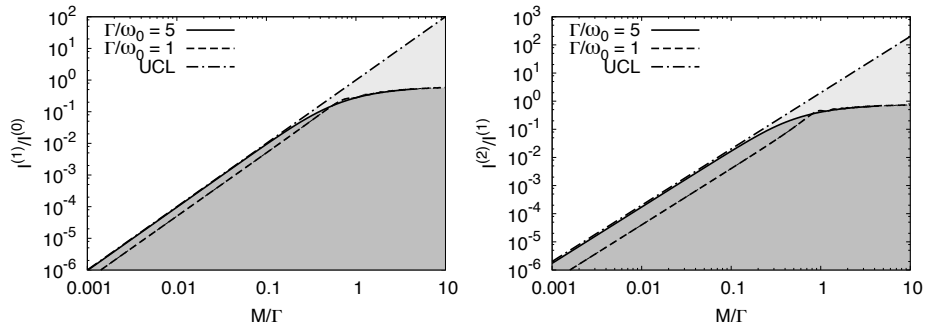


**Figure 7.3:** Relation of the multiple phonon RIXS cross section to the electron-phonon coupling strength $M$ on an absolute energy scale. The ratio of the single-phonon $I^{(1)}$ to zero-phonon $I^{(0)}$ cross section is shown in the left panel. The right panel shows the two-phonon to single-phonon cross section ratio. The curves are universal in the sense that they do not depend on the phonon frequency $\omega_0$ as long as $\Gamma \gg \omega_0$ (for instance, $\Gamma/\omega_0 = 5$). The UCL expansion (straight line) gives accurate results for $M/\Gamma \lesssim 0.2$ and $\Gamma/\omega_0 \gg 1$, *i.e.*, when $\Gamma$ is the dominant energy scale. This corresponds to the physical regime of the e-p interaction at the Cu K edge ($\Gamma \approx 1.5$ eV) and to the intermediate and weak e-p coupling regime at the Cu L edge ($\Gamma \approx 280$) meV.

process contains a viable expansion parameter, which is small even for a fast phonon. The UCL expansion (see Sec. 2.5) formalizes this observation, and the result, obtained in Sec. 7.3.1, is $\mathcal{F}^{(1)}_{\mathrm{UCL}} = T_{\mathrm{el}}(\boldsymbol{\epsilon}', \boldsymbol{\epsilon}) \frac{M}{z^2} \langle f | \sum_i e^{i\mathbf{q}\cdot\mathbf{R}_i} (b_i^\dagger + b_i) | i \rangle$. So, also in this limit, the single-phonon intensity is proportional to $g$.

**Dispersive phonons.** The exact solution of the cross section for Einstein phonons can be generalized to the case of several dispersive phonon branches $\lambda$. The e-p coupling is given by Eq. (7.4). Again we use the canonical transformation [62] $\bar{H} = e^S H e^{-S}$ with $S = \sum_{i,\mathbf{k},\lambda} S_{i\mathbf{k}\lambda}$, where

$$S_{i\mathbf{k}\lambda} = d_i^\dagger d_i \frac{M_{\mathbf{k}\lambda} e^{i\mathbf{k}\cdot\mathbf{R}_i}}{\omega_{\mathbf{k}\lambda}} (b^\dagger_{-\mathbf{k},\lambda} - b_{\mathbf{k}\lambda}). \tag{7.17}$$

so that now

$$\bar{H} = \sum_{\mathbf{k},\lambda} \omega_{\mathbf{k}\lambda} \left( b^\dagger_{\mathbf{k}\lambda} b_{\mathbf{k}\lambda} - g_{\mathbf{k}\lambda} \right), \tag{7.18}$$

with $g_{\mathbf{k}\lambda} = |M_{\mathbf{k}\lambda}/\omega_{\mathbf{k}\lambda}|^2$, and where we assumed that there is a single core hole present. Note that this transformation does not diagonalize the kinetic term for the electrons. However, this is no problem at excitonic edges, where the photo-excited electron is not itinerant, and at the Cu $K$-edge, where the coupling is mediated by the core hole. In close analogy with Eq. (7.12) for the Einstein phonon, this transformation can be inserted in the scattering amplitude:

$$\mathcal{F}_{fi} = T_{\mathrm{el}}(\boldsymbol{\epsilon}', \boldsymbol{\epsilon}) \sum_i e^{i\mathbf{q}\cdot\mathbf{R}_i} \sum_m \frac{\prod_{\mathbf{k},\lambda} \langle n'_{\mathbf{k}\lambda} | \, e^{-S_{i\mathbf{k}\lambda}} \, | n_{\mathbf{k}\lambda}(m) \rangle \langle n_{\mathbf{k}\lambda}(m) | \, e^{S_{i\mathbf{k}\lambda}} \, | n^0_{\mathbf{k}\lambda} \rangle}{z + \sum_{\mathbf{k},\lambda} [g_{\mathbf{k}\lambda} - n_{\mathbf{k}\lambda}(m)] \omega_{\mathbf{k}\lambda}}, \tag{7.19}$$

where $n^0_{\mathbf{k}\lambda}$, $n_{\mathbf{k}\lambda}$, and $n'_{\mathbf{k}\lambda}$ are the occupation numbers of the modes indexed by $\mathbf{k}$ and $\lambda$ in the ground, intermediate, and final states, respectively. Together with the FC factors this is an exact, closed expression for the RIXS response.

We can simplify this expression by assuming that the initial state is close to the ground state, which is a good approximation up to temperatures of the order of 80 meV $\approx$ 930 K for optical phonons in cuprates. Since the FC overlap between the ground and intermediate states follows a Poisson distribution with mean $g_{\mathbf{k}\lambda}$, the scattering channels with largest overlap have small $n_{\mathbf{k}\lambda}(m) - g_{\mathbf{k}\lambda}$. Effectively, we replace

$$z + \sum_{\mathbf{k},\lambda} [g_{\mathbf{k}\lambda} - n_{\mathbf{k}\lambda}(m)] \omega_{\mathbf{k}\lambda} \approx z \prod_{\mathbf{k},\lambda} (1 - [n_{\mathbf{k}\lambda}(m) - g_{\mathbf{k}\lambda}] \omega_{\mathbf{k}\lambda}/z) \tag{7.20}$$

and obtain

$$\mathcal{F}_{fg} \approx \frac{T_{\mathrm{el}}(\boldsymbol{\epsilon}', \boldsymbol{\epsilon})}{z} \sum_i e^{i\mathbf{q}\cdot\mathbf{R}_i} \prod_{\mathbf{k},\lambda} \sum_{n_{\mathbf{k}\lambda}=0}^{\infty} \frac{\langle n'_{\mathbf{k}\lambda} | \, e^{-S_{i\mathbf{k}\lambda}} \, | n_{\mathbf{k}\lambda} \rangle \langle n_{\mathbf{k}\lambda} | \, e^{S_{i\mathbf{k}\lambda}} \, | n^0_{\mathbf{k}\lambda} \rangle}{1 - (n_{\mathbf{k}\lambda} - g_{\mathbf{k}\lambda}) \omega_{\mathbf{k}\lambda}/z}. \tag{7.21}$$

The matrix elements can be evaluated analytically using the displaced harmonic oscillator transformation, resulting in (we suppress the branch index $\lambda$)

$$\mathcal{F}_{fg} \approx T_{\rm el}(\boldsymbol{\epsilon}', \boldsymbol{\epsilon}) \frac{\delta_{\mathbf{q}, \sum_{\mathbf{k}} n'_{\mathbf{k}} \mathbf{k}}}{z} \prod_{\mathbf{k}} \left( \sum_{n=0}^{n'_{\mathbf{k}}} \frac{B_{n'_{\mathbf{k}} n}(g_{\mathbf{k}}) B_{n0}(g_{\mathbf{k}})}{1 - (n - g_{\mathbf{k}})\omega_{\mathbf{k}}/z} + \sum_{n=n'_{\mathbf{k}}+1}^{\infty} \frac{B_{n n'_{\mathbf{k}}}(g_{\mathbf{k}}) B_{n0}(g_{\mathbf{k}})}{1 - (n - g_{\mathbf{k}})\omega_{\mathbf{k}}/z} \right). \tag{7.22}$$

### 7.3.1 UCL expansion of the phonon scattering amplitude

The UCL expansion can be employed to obtain a very compact, approximate expression that is also valid at finite (but low) temperatures. We start from the general case of a dispersive phonon, whose approximate low temperature scattering amplitude (7.21) is expanded as

$$\begin{aligned} \mathcal{F}_{fi} \approx \frac{T_{\rm el}(\boldsymbol{\epsilon}', \boldsymbol{\epsilon})}{z} \sum_i e^{i\mathbf{q}\cdot\mathbf{R}_i} \prod_{\mathbf{k}} \sum_{n_{\mathbf{k}}=0}^{\infty} \langle n'_{\mathbf{k}} | \, e^{-S_{i\mathbf{k}}} \, | n_{\mathbf{k}} \rangle \langle n_{\mathbf{k}} | \, e^{S_{i\mathbf{k}}} \, | n^0_{\mathbf{k}} \rangle \\ \times \sum_{l=0}^{\infty} \left[ (n_{\mathbf{k}} - g_{\mathbf{k}})\omega_{\mathbf{k}}/z \right]^l , \end{aligned} \tag{7.23}$$

which is only valid for $n_{\mathbf{k}}\omega_{\mathbf{k}} < |z|$. For $n_{\mathbf{k}}\omega_{\mathbf{k}} > |z|$, the sum over $l$ diverges independently of the Franck-Condon quenching of the amplitude. Clearly, such a divergence is unphysical: for $n_{\mathbf{k}}$ large, the amplitude should vanish. To avoid this problem, we only retain terms up to the first order in $l$. For high $n_{\mathbf{k}}$, the vanishing Franck-Condon overlap removes any contribution, while for low $n_{\mathbf{k}}$ cutting the expansion is a natural approximation. We get

$$\begin{aligned} \mathcal{F}_{fi} &\approx \frac{T_{\rm el}(\boldsymbol{\epsilon}', \boldsymbol{\epsilon})}{z} \sum_i e^{i\mathbf{q}\cdot\mathbf{R}_i} \prod_{\mathbf{k}} \langle n'_{\mathbf{k}} | \, e^{-S_{i\mathbf{k}}} \left[ 1 + \frac{\omega_{\mathbf{k}}}{z} \left( b^\dagger_{\mathbf{k}} b_{\mathbf{k}} - g_{\mathbf{k}} \right) \right] e^{S_{i\mathbf{k}}} \, | n^0_{\mathbf{k}} \rangle \\ &\approx T_{\rm el}(\boldsymbol{\epsilon}', \boldsymbol{\epsilon}) \frac{M_{\mathbf{q}\lambda}}{z^2} \langle f | \left( b^\dagger_{\mathbf{q}\lambda} + b_{-\mathbf{q},\lambda} \right) | i \rangle \end{aligned} \tag{7.24}$$

to first order in $M_{\mathbf{k}\lambda}/z$, where we neglected terms giving rise to elastic scattering. Again, multi-phonon contributions to $\mathcal{F}_{fi}$ are suppressed as $M_{\mathbf{k}\lambda}/\Gamma$.

This result implies that *momentum dependent RIXS harbors the potential to directly map out the* $\mathbf{q}$ *dependence of the e-p coupling strength* $M_{\mathbf{q}\lambda}$. With this information one can determine, for instance, the spatial range of the e-p interaction $M_{\mathbf{r}\lambda}$: it is simply the Fourier transform of $M_{\mathbf{q}\lambda}$.

Although we showed that the single Einstein phonon cross section is proportional to $g$ in the limit of small $g$ and in the limit of large $\Gamma$, it is in practice near-impossible to measure the absolute RIXS intensity. However, RIXS provides the means to determine the e-p coupling strength $M$ on an absolute energy scale in another way. From the UCL expansion one finds that the ratio of the

one and two-phonon loss amplitude directly reflects the e-p coupling constant: $\mathcal{F}^{(2)}/\mathcal{F}^{(1)} = \sqrt{2}M/z$ in the Einstein phonon case, where we assumed $\Gamma \gg \omega_0, M$. This result is confirmed by the exact solution, see Fig. 7.3. The figure shows the exact curves that relate the (multi-)phonon scattering intensities $I^{(2)}/I^{(1)}$ to the e-p interaction strength $M/\Gamma$ for arbitrary $M$. This method to determine the e-p coupling on an absolute energy scale is particularly powerful in the case of weakly dispersive optical phonons, for instance the much debated phonon modes around 80 meV in the high-$T_c$ cuprates [236–238].

## 7.4 dd excitations dressed by phonons

Hancock *et al.* [239] find that the charge transfer excitation in the zero-dimensional cuprate $CuB_2O_4$ (which is at 6.8 eV) is screened by phonons, explaining the Gaussian line shape of the spectra and yielding a dependence of the charge transfer peak position on the incident energy. In close analogy to their approach, we calculate here the RIXS spectrum of dd excitations that couple to phonons.

Because the scattering process itself is very fast, the lattice has little time to adjust in the intermediate state (as shown in Sec. 7.3) and will approximately be in the same state before and after the scattering process. This is certainly true for small e-p couplings or large core hole lifetime broadenings. The main difference with the preceding sections of this chapter is that the final state has a different charge distribution than the initial state. Therefore, the RIXS process has a lasting influence on the lattice, instead of the transient force when the system returns to its electronic ground state after scattering the photon. The final state corresponds to a displaced oscillator, and the overlap of the initial lattice state with the displaced final states is given by the Franck-Condon factors.

Our starting point is the simple Hamiltonian for a single phonon coupled to a dd excitation (from orbital $\nu'$ to $\nu$[1]):

$$H = \sum_{\mathbf{k}} \left[ \omega_{\mathbf{k}} b^\dagger_{\mathbf{k}} b_{\mathbf{k}} + \sum_i d^\dagger_{i\nu} d_{i\nu} d_{i\nu'} d^\dagger_{i\nu'} e^{i\mathbf{k}\cdot\mathbf{R}_i} M_{\mathbf{k}} \left( b_{\mathbf{k}} + b^\dagger_{-\mathbf{k}} \right) \right] \tag{7.25}$$

We consider RIXS processes where the final state has a single dd excitation, which gets dressed by phonons. The Hamiltonian can be diagonalized as done for dispersive phonons in Sec. 7.3: using $S_{i\mathbf{k}} = d^\dagger_{i\nu} d_{i\nu} d_{i\nu'} d^\dagger_{i\nu'} \frac{M_{\mathbf{k}}}{\omega_{\mathbf{k}}} e^{i\mathbf{k}\cdot\mathbf{R}_i} (b^\dagger_{-\mathbf{k}} - b_{\mathbf{k}})$, we obtain $\bar{H} = \sum_{\mathbf{k}} \omega_{\mathbf{k}} (b^\dagger_{\mathbf{k}} b_{\mathbf{k}} - g_{\mathbf{k}})$.

The RIXS cross section is given by the finite temperature Kramers-Heisenberg equation (2.41). In accordance with the idea that the lattice has no time to respond to the transient charge distribution in the intermediate state, we use the

[1] Each dd excitation has its own e-p coupling $M_{\mathbf{k}} \to M_{\nu'\nu,\mathbf{k}}$. For simplicity, we only consider a single dd excitation here.

UCL expansion to zeroth order:

$$\frac{d^2\sigma}{d\omega d\Omega} \approx \frac{|T_{\rm dd}(\boldsymbol{\epsilon}',\boldsymbol{\epsilon})|^2}{\Gamma^2} \sum_{f,i} e^{-\beta E_i} \left| \langle f| \sum_j e^{i\mathbf{q}\cdot\mathbf{R}_j} d_{j\nu'} d^\dagger_{j\nu} |i\rangle \right|^2 \delta(\omega - E_f + E_i) \quad (7.26)$$

where $T_{\rm dd}(\boldsymbol{\epsilon}',\boldsymbol{\epsilon})$ is the polarization factor (2.42) corresponding to exciting the specific dd excitation ($\nu' \rightarrow \nu$) by two consecutive dipole transitions. The core hole is integrated out. By retaining only the zeroth order of the UCL expansion, the incident energy dependence is lost, and this is different from the work of Hancock *et al.* [239]. In the case of copper $3d^9$, $\nu$ can only assume one value: the photo-excited electron fills the $3d_{x^2-y^2}$ hole and creates a $3d^{10}$ intermediate state. The similarity to the non-resonant inelastic X-ray scattering cross section is striking.

Based on the findings of Ref. [239], we expect the dd excitation to excite many phonons, and consequently we do not care if the initial state has a few phonons already present. For simplicity, we therefore set $T = 0$. For optical phonons, this is in any case a good approximation. Then, we find

$$\langle f| d_{j\nu'} d^\dagger_{j\nu} |i\rangle = \left( \prod_{\mathbf{k}} \langle n'_{\mathbf{k}}, {\rm dd}| \right) e^S d_{j\nu'} d^\dagger_{j\nu} |0\rangle = \prod_{\mathbf{k}} e^{-g_{\mathbf{k}}/2} \frac{\left( \frac{M_{\mathbf{k}} e^{-i\mathbf{k}\cdot\mathbf{R}_j}}{\omega_{\mathbf{k}}} \right)^{n'_{\mathbf{k}}}}{\sqrt{n'_{\mathbf{k}}!}}, \quad (7.27)$$

where $n'_{\mathbf{k}}$ is the number of phonons in the final state with wave vector $\mathbf{k}$, and dd indicates that a dd excitation is present at site $j$ in the final state. Because the final state dd excitation is local, the sum over $j$ in Eq. (7.26) has only one non-zero term, and the $\mathbf{q}$ dependence is lost.

Now we obtain the zero temperature cross section,

$$\begin{aligned} \frac{d^2\sigma}{d\omega d\Omega} &\approx \frac{|T_{\rm dd}(\boldsymbol{\epsilon}',\boldsymbol{\epsilon})|^2}{\Gamma^2} \sum_{f=j,\{n'_{\mathbf{k}}\}} \left| e^{i\mathbf{q}\cdot\mathbf{R}_j} \prod_{\mathbf{k}} \frac{e^{-g_{\mathbf{k}}/2}}{\sqrt{n'_{\mathbf{k}}!}} \left( \frac{M_{\mathbf{k}} e^{-i\mathbf{k}\cdot\mathbf{R}_j}}{\omega_{\mathbf{k}}} \right)^{n'_{\mathbf{k}}} \right|^2 \delta(\omega - E_f) \\ &\approx \frac{N\,|T_{\rm dd}(\boldsymbol{\epsilon}',\boldsymbol{\epsilon})|^2}{\Gamma^2} \prod_{\mathbf{k}} \sum_{n'_{\mathbf{k}}=0}^{\infty} \left( e^{-g_{\mathbf{k}}} \frac{g_{\mathbf{k}}^{n'_{\mathbf{k}}}}{n'_{\mathbf{k}}!} \right) \delta(\omega - E_f) \end{aligned} \quad (7.28)$$

where the final state energy $E_f$ is the dd excitation energy $E_{dd}$ plus the phonon contribution $\sum_{\mathbf{k}} n'_{\mathbf{k}} \omega_{\mathbf{k}}$.

The calculation is easily repeated for local phonons. The result is

$$\frac{d^2\sigma}{d\omega d\Omega} \approx \frac{N\,|T_{\rm dd}(\boldsymbol{\epsilon}',\boldsymbol{\epsilon})|^2}{\Gamma^2} e^{-g} \sum_{n'=0}^{\infty} \frac{g^{n'}}{n'!} \delta(\omega - E_{dd} - n'\omega_0), \quad (7.29)$$

which is a Poisson distribution with phonon number average $g = (M_{dd}/\omega_0)^2$ and variance $\sigma^2 = g$. $M_{dd}$ is the coupling of the dd excitation to phonons. In the limit

of large $g$, it is approximated by a Gaussian distribution. We conclude that the width of the RIXS spectra of dd excitations yields $M_{dd}$ once the phonon energy is known (with an extremely high energy resolution, $\omega_0$ can be measured with RIXS).

In the cuprates, one could study, for instance, the $3z^2$-$r^2$ to $x^2$-$y^2$ dd excitation, which is an intra-$e_g$ transition. The splitting of these levels is partly due to the crystal field of the layered structure, and partly to Jahn-Teller (JT) distortions. Above, we found that the JT contribution is $E_{\mathrm{JT}} = 2M_{dd}$. If we assume that the dd peak broadening is only due to phonons, then the full width at half maximum of the peak directly gives $E_{\mathrm{JT}}$. This way, we can determine what part of the dd excitation energy can be attributed to the JT effect and what part cannot. In practice, other factors also might contribute to the peak width, such as superexchange interactions, and the peak width thus gives only an upper bound to $E_{\mathrm{JT}}$ and $M_{dd}$.

## 7.5 Conclusions

In the analysis above we concentrated on transition metal L edge RIXS, which has the advantage of a photo-electron launched directly into the 3d state. A certain 3d orbital can be selected by choosing the polarization of incident and outgoing X-rays [110], so that the e-p characteristics related to this particular 3d orbital can be measured, as long as the 3d orbital is not fully occupied in the ground state. We extended the theory to include final state dd excitations coupling to the lattice [169], which is of great importance in the study of Jahn-Teller polarons. Also oxygen related phonons can be probed at the O K edge, but as this edge is at lower energy, the photons have less momentum and a smaller part of the BZ can be probed, which is also true for the Cu M edges. As hard X-ray transition metal K edges do not suffer this disadvantage, they provide an even more potent method to measure e-p interactions [230].

The theoretical analysis that we advance here bestows on RIXS the unique potential to provide direct, element-specific and momentum-resolved information on the interaction between electrons and phonons *on an absolute scale*. In weakly correlated electron systems these properties can be computed with modern *ab initio* electronic structure methods, for instance in the newly discovered iron pnictide superconductors [240], and our framework to distill them from RIXS allows a direct comparison. In strongly correlated materials, particularly the high-$T_c$ cuprates, these assets make high resolution RIXS a unique tool to unravel the interaction between its electrons and phonons.

**Acknowledgements.** We thank Lucio Braicovich, Giacomo Ghiringhelli, Tom Devereaux, Brian Moritz and Steven Johnston for fruitful discussions. This work is supported by the U.S. Department of Energy, Office of Basic Energy Sciences under contract DE-AC02-76SF00515 and benefited from the RIXS collaboration

supported by the Computational Materials Science Network (CMSN) program under grant number DE-FG02-08ER46540. This work is supported by the Dutch "Stichting voor Fundamenteel Onderzoek der Materie (FOM).

MvV was supported by the U.S. Department of Energy (DOE), No. DE-FG02-03ER46097. Work at Argonne National Laboratory was supported by the U.S. DOE, Office of Basic Energy Sciences (BES), under contract No. DE-AC02-06CH11357. This research benefited from the RIXS collaboration supported by the Computational Materials Science Network (CMSN), BES, DOE under grant number DE-FG02-08ER46540.